Thermo-optic characterization of KDP single crystals by a modified Sénarmont setup for electro-optic modulation system

H. L. Saadon[1,2*], M. A. Rahma[2], Ali F. Marhoon[2], N. Théofanous[1], and M. Aillerie[3]

[1] *Department of Informatics and Telecommunications, Optoelectronics Group, University of Athens, Panepistimiopolis, Ilisia, GR- 157 84 Athens, Greece*

[2] *Department of Physics, College of Science, University of Basrah, Basrah, Iraq*

[3] *Laboratoire Matériaux Optiques, Photonique et Systémes, UMR CNRS 7132, Université de Metz et Supélec, 2, rue E. Belin, 57070 Metz, France*

[*] *E-mail: haithamsaadon@yahoo.com*

Received March 27, 2009

For our KDP crystal orientation, various thermo-optic (TO) and relevant temperature-dependence parameters are defined, presented, and studied in the framework of a transverse and a longitudinal electro-optic (EO) modulation systems. This study is based on the concept of the so-called opto-electrical bias ($\bar{\varphi}$) applied to the system. For both of the above EO-modulation systems, a set of original equations is extracted and investigated with regard to each of the more important TO or temperature coefficients. Using these equations, for these parameters the role of the transverse configuration is examined in comparison with its corresponding longitudinal configuration. A comparison is done with other orientation of the same KDP crystal.

OCIS code: 250.0250.

doi: 10.3788/COL20090707.0632.

1. Introduction

Thermo-optic (TO) and relevant temperature effects in an intensity-modulation (IM) electro-optic (EO) system may strongly affect the EO response of a crystal[1−3]. In the entire EO-modulation system, these effects can be examined via their influence on the position and thermal stability of the operating point over the system's characteristic (transfer) curve[3]. Under these conditions, the concept and the role of the applied optical and electrical bias may be important[4].

We present a novel consideration of the EO and TO effects which are made on the basis of the combined opto-electrical (optical and electrical) bias and the corresponding thermal stability along the aforementioned transfer curve. In this framework, our interest is focused on the TO behaviour of an EO modulator crystal as it is expressed by the influence of temperature T on the crystal's optical or electro-optical quantities such as the refractive indices, n_0 and n_e, the effective EO coefficient r, the spontaneous birefringence $\Delta n^{(0)}$, the half-wave voltage V_π, the optical phase retardation Γ, and the intensity-modulation (IM) depth m of the entire EO-modulation system. After stating the appropriate definitions of the corresponding thermo-optic and temperature coefficients, we derive and present useful original equations connecting these parameters when either a transverse or a longitudinal configuration is used in the IM EO-modulation system. Then, we present investigations of these equations as regards the above parameters in the determination of temperature coefficients for the effective EO coefficient r, the half-wave voltage V_π, and the IM depth m.

Incited by the above, we make a modified Sènarmont system to study experimentally the electro-optic and relevant temperature effects in 45° X-cut and 45° Y-cut KH_2PO_4 (or KDP) crystals of various configurations. The above measurements are performed using accurate and precise methods such as the frequency-doubling EO-modulation (FDEOM) method and the modulation depth (MDM) method[5,6]. Finally, these results are compared with each other and another orientation of the same crystal.

2. Experimental system and methods

The EO and TO measurements were performed by a modified Sénarmont setup. Figure 1 shows the arrangement of the optical and electronic components. The EO crystal sample S is placed between a polarizer P and a quarter-wave plate Q, the neutral axes of which are oriented at 45° from the axes of the crystal and the polarizer. Behind the quarter-wave plate, a rotating analyzer

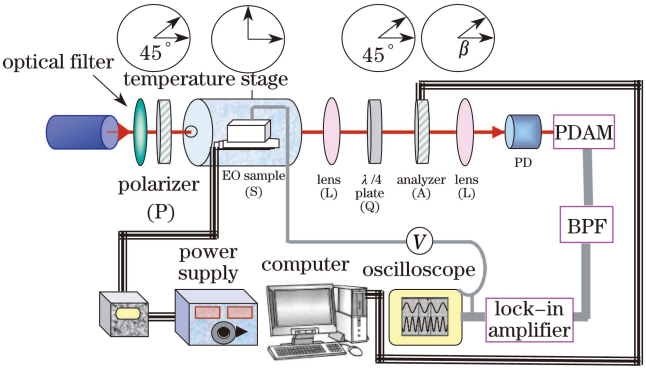

Fig. 1. Schematic diagram for measuring EO and TO parameters in the modified Sénarmont system.

A is free to be positioned at any azimuthal angle $\hat{\beta}$. The electric field is applied to the sample by means of a voltage V. As a result, when a laser beam passes through the system, it is transformed into an intensity-modulated beam. This modulated beam is received by a photodetection system. The photodetection system consists of a photodiode (PD) and its associated high-gain photodiode amplifier (PDAM) followed by a band-pass filter (BPF). The output voltage of the entire photodetection system is conveyed to an oscilloscope. For increasing and improving the sensitivity of the method, we use a lock-in amplifier. Finally, for TO measurements, a temperature stage is designed and built to fit the optical setup.

In general, for systems of the above kind, the transfer function of the transmitted laser light intensity I can be expressed as $I=f(\bar{\varphi})$, where $\bar{\varphi}$ is a quantity called the opto-electrical bias of the system and defined by[3]

$$\bar{\varphi} = \Gamma - 2\hat{\beta} \ . \tag{1}$$

More precisely, for systems such as those shown in Fig. 1, the transfer function becomes[3,6]

$$T = \frac{T_0}{2}\left(1 - \sin\bar{\varphi}\right) \ , \tag{2}$$

where T_0 is the transmission factor of the system.

In what follows, the crystal sample is assumed linearly EO and therefore in the presence of an applied electric field $E=V/d$ (where V is the applied voltage and d the electrode spacing) to an EO crystal, the total birefringence of the crystal can be expressed by the linear approximation[6,7]

$$\Delta n = \Delta n^{(0)} - \frac{1}{2}n^3 rE = \Delta n^{(0)} - \frac{n^3 r}{2d}V \ , \tag{3}$$

where $\Delta n^{(0)}$ is the natural or spontaneous birefringence, r represents the effective EO coefficient, and n is the effective refractive index of the sample given by

$$n = \left(\frac{2n_0^2 n_e^2}{n_0^2 + n_e^2}\right)^{1/2} \ . \tag{4}$$

The corresponding total differential phase shift or relative refraction is given by[4,8−10]

$$\Gamma = \left(\frac{2\pi L}{\lambda_0}\right)\Delta n \ , \tag{5}$$

where L is the length of the crystal (along the laser beam) and λ_0 is the wavelength of the laser beam in vacuum. For the field-induced optical phase retardation, the expression is

$$\Gamma_E = \left(\frac{\pi}{\lambda_0}\right) Ln^3 rE = \pi\left(\frac{V}{V_\pi}\right) \ , \tag{6}$$

where

$$V_\pi = \frac{\lambda_0}{n^3 r}\left(\frac{d}{L}\right) \tag{7}$$

is the half-wave voltage of the crystal sample for the configuration under consideration.

Hence, in the case of a transverse EO modulator, the half-wave voltage of the sample will be proportional to the dimension ratio d/L. Accordingly, in the transverse EO-modulation system under consideration, the half-wave voltage of the sample could be considerably reduced if d is taken significantly smaller than L and moreover, it would be more or less affected by the thermal expansion effects in the crystal. By contrast, for the longitudinal configuration, we have $L=d$ and therefore the half-wave voltage of the crystal is independent on its dimensions, and their thermal expansions depends only on the thermo-optic effects modifying the refractive index and the EO coefficient of the crystal.

When a system such as the one shown in Fig. 1 is used for either a transverse or a longitudinal IM electro-optic modulation, the I-$\bar{\varphi}$ curve representing the transfer function according to Eq. (2) can be taken as the characteristic curve of the system (Fig. 2).

As can be seen from Eqs. (1)−(6), the position of the quiescent point on this characteristic curve is controlled by the opto-electrical bias $\bar{\varphi}$ and can be established by adjusting either the azimuthal angle $\hat{\beta}$ of the analyzer (optical bias) or/and the applied electric direct current (DC) voltage $V=V_{\rm DC}$ (electrical bias) which controls the static retardation $\bar{\Gamma} = \Gamma^{(0)} + \Gamma_{\rm DC}$, where $\Gamma^{(0)} = (2\pi L/\lambda)\,\Delta n^{(0)}$ is the natural phase retardation and $\Gamma_{\rm DC} = \pi(V_{\rm DC}/V_\pi)$ is the DC-bias phase retardation. According to Eq. (1), the total opto-electrical bias will be given by

$$\bar{\varphi} = \overline{\Gamma} - 2\hat{\beta} = \Gamma^{(0)} + \pi\left(V_{\rm DC}/V_\pi\right) - 2\hat{\beta} \ . \tag{8}$$

It is known that one of the more important quiescent points along the I-$\bar{\varphi}$ characteristic curve is the minimum-transmission point, M_0, for which the derivative of $f(\bar{\varphi})$ is zero. On the assumption of validity of Eq. (2), along with Eq. (8), it is easily proven that this point corresponds to a total opto-electrical bias $(\bar{\varphi} = \varphi_0 = (1/2 + 2k)\pi$ $(k = 0, \pm1, \cdots)$ and is attained when the condition $\Gamma^{(0)} + (V_{\rm DC}/V_\pi - 1/2{-}k)\pi = \hat{\beta}$ is met. This point is also called the double-frequency point, because if an alternating current (AC) field of frequency ν is applied to the crystal, a clear signal modulated at a frequency of 2ν appears at the demodulated output[5,6]. The double-frequency point can be used to measure the half-wave voltage V_π and the effective EO coefficient r by means of a FDEOM method using the system in Fig. 1[5,6]. The double frequency

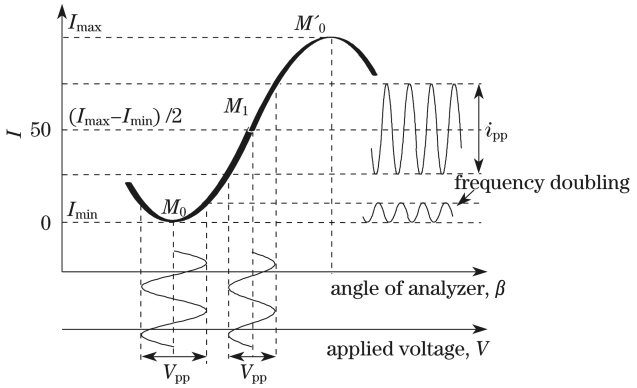

Fig. 2. Optical transmission of the system as a function of the analyzer angle $\hat{\beta}$ or the applied voltage V.

signal is lost as a step of a DC electric field applied to the crystal and can be recovered if the analyzer is rotated by an angle given by

$$\Delta\hat{\beta} = \frac{\Delta\bar{\Gamma}}{2} = \left(\frac{\pi L}{2\lambda}\right) n^3 r \Delta E. \tag{9}$$

Another important quiescent point is the middle point M_1 corresponding to the mid-point intensity I=$I_0/2$ of the transfer function (Fig. 2). This point is also called the maximum-linearity point, because if an AC field of frequency ν is applied to the crystal, a clear signal modulated at the same frequency ν appears at the demodulated output[5]. On the assumption of Eq. (2), along with Eq. (8), it is easily proven that the maximum-linearity point corresponds to a total opto-electrical bias $\bar{\varphi} = \varphi_1 = k\pi$ ($k = 0, \pm1, \cdots$) and is attained when the condition $\Gamma^{(0)} + (V_{\rm DC}/V_\pi)\pi = 2\beta$ is met. The so-called linear working point M_1 can be used to determine the EO coefficient as a function of frequency by means of modulation-depth method (MDM)[5]. Measuring the peak-to-peak amplitude $i_{\rm pp}$ of the modulated signal at the point M_1, one can obtain the EO coefficient directly from[5,11]

$$r(\nu) = \left(\frac{\lambda d}{\pi n^3 L V_{\rm m}}\right) \frac{i_{\rm pp}}{I_0}, \tag{10}$$

where $V_{\rm m}$ is the amplitude of the AC field and $I_0 = I_{\max} - I_{\min}$ represents the total intensity shift of the transfer function. In Eq. (10), the dimensionless ratio $i_{\rm pp}/I_0$ is commonly noted as m and called the IM depth.

3. Relationships between TO parameters of EO interest

In an EO-modulation system, various TO parameters exist which refer to the temperature dependence of useful quantities interconnected in the framework of the system. To define these parameters, we have adopted the definition of p=du/dT for the TO coefficient and

$$q = \left(\frac{1}{u}\right)\left(\frac{{\rm d}u}{{\rm d}T}\right), \tag{11}$$

for the corresponding temperature coefficient of a temperature quantity u[3]. On the other hand, as Γ depends on various EO and TO parameters, the thermal stability of the opto-electrical bias $\bar{\varphi} = \overline{\Gamma} - 2\hat{\beta}$ will depend on the values of these parameters.

For the case of the typical Sénarmont-type transverse EO-modulation system, it has been proven that the following set of equations is valid for the EO and TO parameters for any operating point of the system[3]

$$n_1 n_2 (\beta_2 - \beta_1) = \bar{n}\Delta n^{(0)} (\mu_\Delta - \overline{\mu}), \tag{12a}$$

$$\kappa = \frac{{\rm d}\overline{\Gamma}}{{\rm d}T} = \Gamma^{(0)} (\mu_\Delta + \alpha_{\rm L}) - \pi\delta\left(\frac{V_{\rm DC}}{V_\pi}\right), \tag{12b}$$

$$\rho = \frac{1}{r}\left(\frac{{\rm d}r}{{\rm d}T}\right) = -(\delta + 3\beta) + (\alpha_{\rm d} - \alpha_{\rm L}), \tag{12c}$$

$$\xi_{\rm m} = \frac{1}{m}\left(\frac{{\rm d}m}{{\rm d}T}\right) = (\rho + 3\beta) - (\alpha_{\rm d} - \alpha_{\rm L}), \tag{12d}$$

where ρ, δ, μ_Δ, and $\xi_{\rm m}$ are the temperature coefficients for the effective EO coefficient r, the half-wave voltage V_π, the spontaneous birefringence $\Delta n^{(0)}$, and the IM depth m, respectively. For example, we defined the following coefficients:

$$\delta = \frac{1}{V_\pi}\left(\frac{{\rm d}V_\pi}{{\rm d}T}\right),$$
$$\mu_\Delta = \frac{1}{\Delta n^{(0)}}\left(\frac{{\rm d}\Delta n^{(0)}}{{\rm d}T}\right),$$
$$\xi_{\rm m} = \frac{1}{m}\left(\frac{{\rm d}m}{{\rm d}T}\right) = -\delta, \tag{13}$$

where ${\rm d}V_\pi/{\rm d}T$, ${\rm d}\Delta n^{(0)}/{\rm d}T$, and ${\rm d}m/{\rm d}T$ are the thermo-optic coefficients for V_π, $\Delta n^{(0)}$, and m, respectively. As to the temperature coefficients $\alpha_{\rm L}$ and $\alpha_{\rm d}$ for the crystal length L and the crystal thickness d, respectively, they are given by

$$\alpha_{\rm L} = \frac{1}{L}\left(\frac{{\rm d}L}{{\rm d}T}\right),$$
$$\alpha_{\rm d} = \frac{1}{d}\left(\frac{{\rm d}d}{{\rm d}T}\right), \tag{14}$$

where ${\rm d}L/{\rm d}T$ and ${\rm d}d/{\rm d}T$ are the thermal expansion coefficients of the crystal along the directions L and d, respectively. Also, the temperature coefficients of the refractive indices n, n_1=n_0, and n_2=$n_{\rm e}$, are defined by

$$\beta = \frac{1}{n}\left(\frac{{\rm d}n}{{\rm d}T}\right),$$
$$\beta_1 = \beta_0 = \frac{1}{n_0}\left(\frac{{\rm d}n_0}{{\rm d}T}\right),$$
$$\beta_2 = \beta_{\rm e} = \frac{1}{n_{\rm e}}\left(\frac{{\rm d}n_{\rm e}}{{\rm d}T}\right), \tag{15}$$

where ${\rm d}n/{\rm d}T$, ${\rm d}n_0/{\rm d}T$, and ${\rm d}n_{\rm e}/{\rm d}T$ represent the corresponding thermo-optic coefficients. Also, $\beta = \beta_0$ and β=$\beta_{\rm e}$ stand for r_{63} and r_{41} EO coefficients, respectively. Lastly, $\bar{n} = (1/2)(n_1 + n_2)$ is the mean refractive index and κ represents the thermo-optic coefficient ${\rm d}\overline{\Gamma}/{\rm d}T$ of the static phase retardation $\bar{\Gamma}$.

Similar calculations made in the case of a Sènarmont-type longitudinal EO-modulation system are shown as Eqs. (12a) and (12b), which refer to the difference (β_2−β_1) and the thermo-optic coefficient κ of $\bar{\Gamma}$, respectively, and are the same in the both transverse and longitudinal EO systems. By contrast, Eqs. (12c) and (12d), which refer to the temperature coefficients ρ and $\xi_{\rm m}$, respectively, differ in these two opto-geometric configurations by the thermal expansion term ($\alpha_{\rm d}$−$\alpha_{\rm L}$). According to Eq. (7), it can be proven (see Appendix A) that the temperature coefficient ρ is ruled by the formula

$$\rho = \frac{1}{r}\left(\frac{{\rm d}r}{{\rm d}T}\right) = -(\delta + 3\gamma), \tag{16}$$

where γ is the coefficient (see Appendix B) ruled by

$$\gamma = \frac{\beta_0 n_{\rm e}^2 + \beta_{\rm e} n_0^2}{n_0^2 + n_{\rm e}^2}. \tag{17}$$

Table 1. Description of the Electro-Optical Configuration Used in Our Experiments on KDP Crystals

Symmetry-EO Tensor	EO Coefficient	Transverse Configuration	Longitudinal Configuration
$\bar{4}2m$			
$\begin{bmatrix} 0 & 0 & 0 \\ 0 & 0 & 0 \\ 0 & 0 & 0 \\ r_{41} & 0 & 0 \\ 0 & r_{52} & 0 \\ 0 & 0 & r_{63} \end{bmatrix}$	r_{63}	$\mathbf{E}//Z$ and $\mathbf{K}//Y$	-
	r_{41}	$\mathbf{E}//X$ and $\mathbf{K}//Y$	$\mathbf{E}//X$ and $\mathbf{K}//X$

From Eq. (16) and the third line of Eq. (13), the temperature coefficient ξ_{m} will be given by

$$\xi_{\mathrm{m}} = \frac{1}{m}\left(\frac{\mathrm{d}m}{\mathrm{d}T}\right) = \rho + 3\gamma. \tag{18}$$

It is to be emphasized that, as seen from the above sets of equations, Eqs. (12c) and (16), which refer to the temperature coefficient ρ, and Eqs. (12d) and (18), which refer to the temperature coefficient ξ_{m}, differ by the thermal expansion term $(\alpha_{\mathrm{d}}-\alpha_{\mathrm{L}})$, which is absent in a longitudinal EO-modulation system. This fact may be advantageous for such a longitudinal system if the thermal expansion contribution is high in the corresponding transverse EO-modulation system.

4. Experimental results

The measurements are performed on the KDP crystal grown with the water solution by slow evaporation technique. We adopt three sample cuts to explore two different configurations. The first and second cuts are 4×10×4 (mm) 45° Y-cut and 5×10×4 (mm) Y-cut KDP crystals for the transverse EO coefficients r_{63} and r_{41}, respectively. The third one is 10×5×4 (mm) 45° X-cut KDP crystal involving the longitudinal EO coefficient r_{41}. For each sample, the dimension along the laser beam propagation is 10 mm. Table 1 summarizes the configurations (directions of the light propagation and the applied electric field and EO coefficient involved) that are studied.

Electro-optical and thermo-optical measurements were carried out using a 15-mW He-Ne laser (λ=633 nm) with 1-kHz AC voltage up to 300-V peak to peak and a DC voltage with amplitude varying between −300 and 300 V.

4.1 Electro-optical measurements

We firstly determined the quantities r_{63}, r_{41}, and V_π using the FDEOM method with the transverse configuration. Figure 3, for transverse configuration, describes the frequency-doubling azimuthal angle $\hat{\beta}$ of the analyzer as a function of the DC voltage V_{DC}. To reduce the effect of random errors, the data was fitted by linear least-squares, which led to straight lines. Using the slopes $\delta\beta/\delta V_{\mathrm{DC}}$ of the above curves in Eq. (9), we determined the EO coefficients r_{63} and r_{41}, respectively. So, for r_{63}, we obtained the static DC value of r_{63}=11.4 pm/V and the half-wave voltage V_π of 6.47 kV. Also, we found the static EO coefficient r_{41} and the half-wave voltage V_π with values equal to 8.67 pm/V and 9.24 kV, respectively.

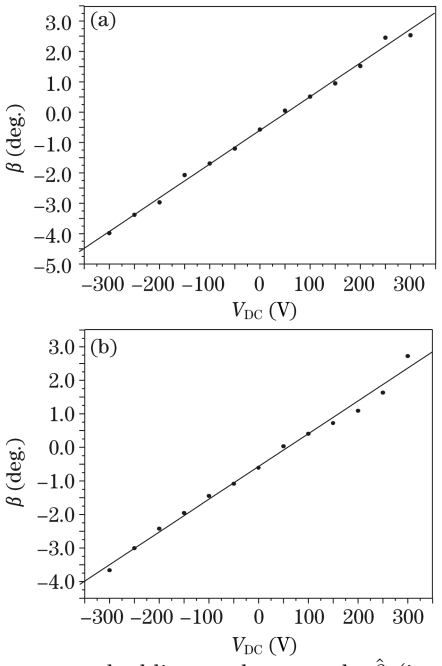

Fig. 3. Frequency-doubling analyzer angle $\hat{\beta}$ (involving the transverse configuration) induced by a DC applied voltage V_{DC} for (a) r_{63} configuration and (b) r_{41} configuration.

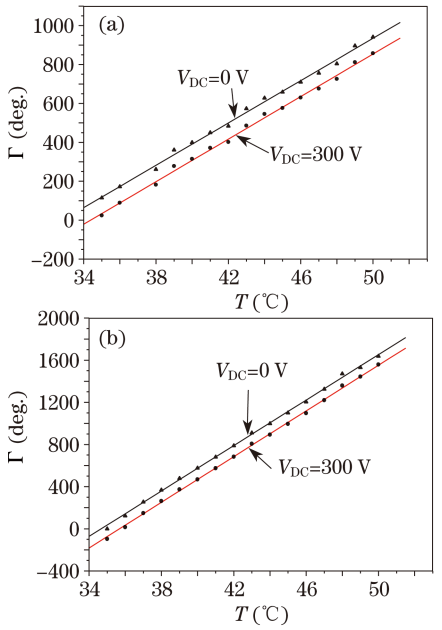

Fig. 4. Temperature dependence of the static phase retardation $\bar{\Gamma}$ for two different DC voltages for (a) r_{63} transverse configuration and (b) r_{41} transverse configuration.

4.2 Thermo-optical measurements

Thermo-optical measurements are important when one uses these crystals orientation in an EO modulation system. So, the optical system in Fig. 1 was upgraded to allow for varying temperature among the crystals measured. An accurate and precise feedback controlled heater was used and the temperature was monitored with a digital thermometer with ±0.05 °C accuracy.

First, to investigate the TO behaviour of our orientation 45° Y-cut KDP crystal with the transverse configuration, by means of the FDEOM method, we

plotted the phase retardation $\bar{\Gamma}$ as a function of temperature T for two different DC voltages of V_{DC}=0 and V_{DC}=300 V in Fig. 4. The continuous curves in this figure represent the graphical plots of the linear least-square, which fit to the experimentally obtained data points.

Next, it was important to define the thermal stability of the spontaneous birefringence $\Delta n^{(0)}$ of the crystal expressed by the TO coefficient $\mathrm{d}\Delta n^{(0)}/\mathrm{d}T$ in used configuration and then, using Fig. 4, we determined the temperature coefficient μ_Δ. For this purpose, we firstly extracted the TO coefficient $\kappa = \mathrm{d}\bar{\Gamma}/\mathrm{d}T$ or the slopes of the straight lines on the voltages from Fig. 4. As expected, the $\kappa - V_{DC}$ curves are straight lines. After applying the linear least-squares fitting on the values of κ, we determined the interception of the curves with values equal to −54.59 deg./°C and 108.26 deg./°C for r_{63} and r_{41} configurations, respectively. Second, using the value of $\Gamma^{(0)}$ as described above and the value of thermal expansion α_L[12] in Eq. (12b), we found the temperature coefficients μ_Δ=−243.015×10^{-6} °C^{-1} and −479.43×10^{-6} °C^{-1} for r_{63} and r_{41} configurations, respectively. Then, using the second of line Eq. (13) with $\Delta n^{(0)}=n_e-n_0=-0.04$[13], we determined the TO coefficients $\mathrm{d}\Delta n^{(0)}/\mathrm{d}T$ of the r_{63} and r_{41} configurations, respectively, which were equal to 9.72×10^{-6} °C^{-1} and 19.17×10^{-6} °C^{-1}.

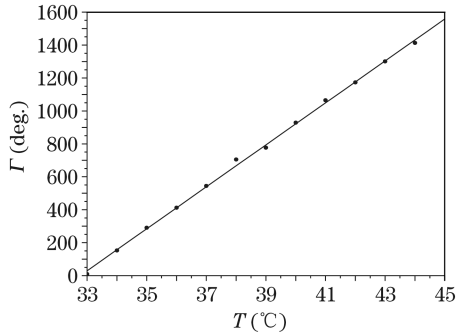

Fig. 5. Temperature dependence of the static phase retardation $\bar{\Gamma}$ at V_{DC}=0 for the longitudinal configuration involving the EO coefficient r_{41}.

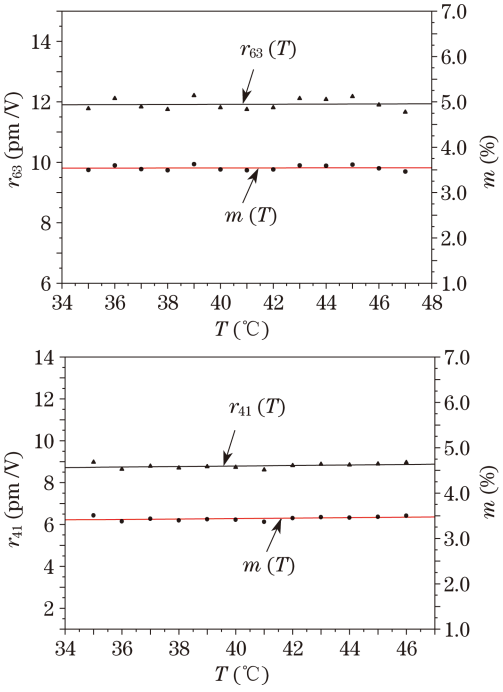

Fig. 6. Temperature dependences of the transverse EO coefficient r and the IM depth m for (a) r_{63} configuration and (b) r_{41} configuration.

In the case of the longitudinal configuration, we recorded the dependence of the phase retardation $\bar{\Gamma}$ on the temperature T in r_{41} configuration at V_{DC}=0. Typical results obtained in 45° X-cut KDP crystal are shown in Fig. 5. A least-square fitting of the data to a straight line reveals a good linearity leading to a slope $\mathrm{d}\Gamma^{(0)}/\mathrm{d}T$=127.41 deg./°C and a TO coefficient according to $\mathrm{d}\Delta n^{(0)}/\mathrm{d}T$=22×10^{-6} °C^{-1}. Then, using the second line of Eq. (13), we determined the temperature coefficient μ_Δ of −550×10^{-6} °C^{-1} for r_{41} longitudinal configuration.

Figure 6 shows, by means of Eq. (10), the temperature dependence of the r_{63} and r_{41} transverse EO coefficients obtained via the MDM method. These curves exhibit small temperature dependent oscillations of r_{63} and r_{41} around the mean values of r_{63} and r_{41}, respectively. From the central line of the curves, by means of a linear least-squares fit to the so-obtained data, it can be found that the coefficients r_{63} and r_{41} equal to 11.8 pm/V and 8.72 pm/V, respectively. Also, from the slopes in Fig. 6, we extracted the TO coefficients $\mathrm{d}r_{63}/\mathrm{d}T$ =2.1×10^{-3} pm/(V·°C) and $\mathrm{d}r_{41}/\mathrm{d}T$ =12.31×10^{-3} pm/(V·°C). Using these results in the first line of Eq. (12c), we determined for r_{63} and r_{41}, the temperature coefficients of ρ=0.177×10^{-3} °C^{-1} and ρ=1.414×10^{-3} °C^{-1}, respectively.

To evaluate the TO behavior of KDP crystal when used as a modulator crystal in a typical IM system, it is useful to find the temperature dependence of the IM depth m. Precisely, by applying the MDM method and the results of r-T curves presented in Fig. 6 and then, using Eq. (10), we determined the m-T curves in Fig. 6. From the linear-fit straight line, a modulation depth of m=3.5% and 3.41% and a thermo-optic coefficient $\mathrm{d}m/\mathrm{d}T$=6.23×10^{-6} °C^{-1} and 48.14×10^{-6} °C^{-1} can be obtained for transverse configurations r_{63} and r_{41}, respectively. Using these values in the third line of Eq. (13), the temperature coefficients ξ_m=0.177×10^{-3} °C^{-1} and 1.407×10^{-3} °C^{-1}, respectively, for r_{63} and r_{41} configurations, can be extracted. According to Eq. (12d) and the values of ξ_m for configurations r_{63} and r_{41}, respectively, we found the temperature coefficients of δ=−0.177×10^{-3} °C^{-1} and −1.407×10^{-3} °C^{-1}.

Also, by using Eq. (10), we determined the temperature dependence of the r_{41} longitudinal EO configuration with the MDM method. The results are shown in Fig. 7. From this figure, we also see the small temperature dependent undulations of r_{41} around the mean value of r_{41}. A least-square fit to these values of r_{41} leads to straight line described in this Figure. From this line, we extracted an EO coefficient r_{41} =8.36 pm/V and from its slope, a thermo-optic coefficient equal to 12.97×10^{-3} pm/(V·°C). Then, using these values in the first line of Eq. (16), we found the temperature coefficient for r_{41} of ρ= 1.548×10^{-3} °C^{-1}.

In addition, for longitudinal configuration, we present

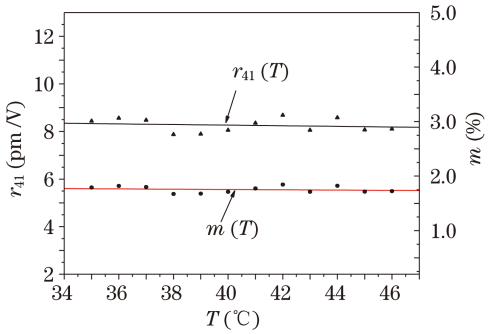

Fig. 7. Temperature dependences of the EO coefficient r_{41} and the IM depth m for the longitudinal configuration.

the temperature dependence of the IM depth m deduced from the r_{41}-T curve. Using Eq. (10), the so-obtained results are illustrated in Fig. 7. After applying a linear least-square fit to the values of m, we can find from this line the modulation depth of m=1.76% and the corresponding TO coefficient of $\mathrm{d}m/\mathrm{d}T$ =27.51×10^{-6} °C^{-1}. Using these values in the third line of Eq. (13), a temperature coefficient ξ_{m}=1.563×10^{-3} °C^{-1} can be extracted for IM depth m. Consequently, according to Eq. (18), a temperature coefficient δ for V_π is found to be −1.563×10^{-3} °C^{-1}.

The temperature coefficients β_0 and β_{e} of the ordinary and extraordinary refractive indices n_0 and n_{e}, respectively, for r_{63} and r_{41} transverse configurations, are calculated. Using Eq. (12c) or (12d) and the values of ρ, ξ_{m}, and δ presented in above and the thermal expansions α_{L} and α_{d} reported in Ref. [12], the values of β_0 and β_{e} are found equal to 2.6×10^{-6} °C^{-1} for r_{63} configuration and 0.45×10^{-6} °C^{-1} for r_{41} configuration, respectively, while the corresponding TO coefficient $\mathrm{d}n_0/\mathrm{d}T$ and $\mathrm{d}n_{\mathrm{e}}/\mathrm{d}T$ can be obtained to be 3.92×10^{-6} °C^{-1} and 0.66×10^{-6} °C^{-1} for r_{63} and r_{41} configurations, respectively. Also, from the equations $\mathrm{d}n_{\mathrm{e}}/\mathrm{d}T$=$\mathrm{d}n_0/\mathrm{d}T$+$\mathrm{d}\Delta n^{(0)}/\mathrm{d}T$ and $\mathrm{d}n_0/\mathrm{d}T$=$\mathrm{d}n_{\mathrm{e}}/\mathrm{d}T$−$\mathrm{d}\Delta\mathrm{n}^{(0)}/\mathrm{d}T$, we extract the TO coefficients $\mathrm{d}n_{\mathrm{e}}/\mathrm{d}T$ and $\mathrm{d}n_0/\mathrm{d}T$ of n_{e} and n_0, which are equal to 13.64×10^{-6} °C^{-1} and −18.5×10^{-6} °C^{-1} for r_{63} and r_{41} configurations, respectively. From these values in Eq. (15), the temperature coefficients β_{e} and β_0, for r_{63} and r_{41} configurations, are found equal to 9.28×10^{-6} °C^{-1} and −12.27×10^{-6} °C^{-1}, respectively. Then, by means of Eq. (12a) with n_1=n_0 and n_2=n_{e}, the differences $\mu_\Delta - \bar{\mu}$ between the temperature coefficients of the birefringence $\Delta n^{(0)}$ and the mean refractive index $\bar{n}$, for r_{63} and r_{41} configurations, are obtained to be −0.248×10^{-3} °C^{-1} and −0.473×10^{-3}, respectively.

In the longitudinal configuration, using Eq. (18), the coefficient γ is found to be (1/3)(ξ_{m} − ρ)=5×10^{-6} °C^{-1}. So, from the expression of birefringence $\Delta n^{(0)}$=n_{e}−n_0 and Eq. (15), the temperature coefficient can be obtained to be β_0 = [$\gamma(n_0^2 + n_{\mathrm{e}}^2)$ − (n_0^2/n_{e})($\mathrm{d}\Delta n^{(0)}/\mathrm{d}T$)]/($n_0^3$+$n_{\mathrm{e}}^3/n_{\mathrm{e}}$)=−2.663×10^{-6} °C^{-1}; hence, the corresponding TO coefficient will be $\mathrm{d}n_0/\mathrm{d}T$=$\beta_0 n_0$=−4.015×10^{-6} °C^{-1}. Then, the TO coefficient of n_{e} can be calculated from the formula $\mathrm{d}n_{\mathrm{e}}/\mathrm{d}T$=$\mathrm{d}\Delta n^{(0)}/\mathrm{d}T$+$\mathrm{d}n_0/\mathrm{d}T$=17.984×10^{-6}°C^{-1}; hence, the corresponding temperature coefficient will be β_{e}=(1/n_{e})($\mathrm{d}n_{\mathrm{e}}/\mathrm{d}T$)=12.257×10^{-6} °C^{-1}. In addition, from Eq. (12a), the coefficient Δ_μ can be calculated to be Δ_μ = μ_Δ − $\bar{\mu}$ = ($n_0 n_{\mathrm{e}}/\bar{n}\Delta n^{(0)}$)($\beta_{\mathrm{e}}$ − β_0)=−0.554×10^{-3} °C^{-1}.

5. Discussion and investigation

The results obtained for transverse and longitudinal configurations are summarized in Table 2. For transverse configuration, we measured the EO coefficients r_{63}=11.4 pm/V and 11.8 pm/V and r_{41}=8.67 pm/V and 8.72 pm/V, respectively, by a modified Sènarmont system using two methods, namely the FDEOM and MDM methods. Hence, we notice that these coefficients are very close to one another (within experimental errors) and similar to the results reported in Ref. [14]. Obviously, this fact constitutes comparative evidence that our system is correct and effective. But, for longitudinal configuration, using the MDM method, we find that the EO coefficient r_{41} are in good concordance with the value reported in Ref. [14].

Additional evidence of the system under consideration comes from its ability to detect the undulation in the temperature dependence curves, r-T, of Figs. 6 and 7. Such as a small undulation of EO coefficients is due to the interactions of the crystal's thermal expansion with multiple beam interference and TO effects[16,17].

To evaluate the thermal instability of spontaneous birefringence for our crystal orientation, which is expressed by the coefficient of thermal variation or TO coefficient $\mathrm{d}\Delta n^{(0)}/\mathrm{d}T$, it is useful to compare it with those of an other orientation (45° Z-cut KDP)[18]. This crystal orientation is chosen as a reference for comparison, particularly in EO systems. We adopt and insert in Table 2 for the coefficient $\mathrm{d}\Delta n^{(0)}/\mathrm{d}T$ of this crystal orientation the value 15×10^{-6} °C^{-1} of Ref. [18]. But, for our KDP crystal we find this coefficient equal to 9.72×10^{-6} °C^{-1}, which is in good agreement with the results obtained in Ref. [19]. This is smaller than the corresponding value of other crystal orientation (45° Z-cut). That means our results show a more powerful temperature control which would be possibly required for 45° Z-cut KDP crystal.

From the results of calculations that leads to Figs. 6 and 7, it can be deduced that the values of r, m, and the forms of the corresponding temperature dependences show small oscillations of EO coefficients, r_{63} and r_{41}, and modulation depth m around the mean value of them. Indeed, our crystal orientation is nearly insensitive to the temperature. For the sake of comparison, from the straight line fitted to the experimental data in the r_{63}-T diagram of Ref. [18], we extract different temperature and TO coefficients. The so-obtained coefficients are shown in Table 2. From this table, it is deduced that the TO parameters in our results are smaller than that of other crystal orientation. Moreover, in our crystal the thermal instability of the IM depth in the r_{63} configuration, as expressed by the temperature coefficient ξ_{m}, proves to be much lower than other crystal orientation, and therefore no specific thermal control is indispensable.

In investigation, we firstly dealt with the difference $\mu_\Delta - \bar{\mu}$ between the temperature coefficients of the birefringence $\Delta n^{(0)}$ and the mean refractive index $\bar{n}$, which are ruled by Eq. (12a). It is again to be emphasized that, irrespective of the chosen EO-modulation configuration (transverse and longitudinal) these parameters are nearly the same.

Table 2. EO and TO Parameters Measured in Our KDP Crystal Orientation and Extracted from Literature of Other Orientations of the Same Crystal (45° Z-cut KDP)

Parameters		Transverse Configuration			Longitudinal Configuration
		Our Orientation Measured Values	Values from Literatures	Other Orientations from Literatures	Our Orientation Measured Values
r (pm/V)	r_{63}	11.4, 11.8	11 [14]	11.8[18]	-
	r_{41}	8.67, 8.72	8[14], 8.6[15]	-	8.36
$\mathrm{d}\Delta n^{(0)}/\mathrm{d}T$ ($^\circ\mathrm{C}^{-1}$)	r_{63}	9.72×10^{-6}	11×10^{-6}[19]	15×10^{-6}[18]	-
	r_{41}	19.17×10^{-6}	-	-	22×10^{-6}
$\mathrm{d}r/\mathrm{d}T$ (pm/V °C)	r_{63}	2.10×10^{-3}	-	0.08[18]	-
	r_{41}	12.31×10^{-3}	-	-	12.97×10^{-3}
μ_Δ ($^\circ\mathrm{C}^{-1}$)	r_{63}	-243.01×10^{-6}	-	-375×10^{-6}[18]	-
	r_{41}	-479.43×10^{-6}	-	-	-550×10^{-6}
ρ ($^\circ\mathrm{C}^{-1}$)	r_{63}	0.177×10^{-3}	-	6.7×10^{-3}[18]	-
	r_{41}	1.414×10^{-3}	-	-	1.548×10^{-3}
ξ_m ($^\circ\mathrm{C}^{-1}$)	r_{63}	0.177×10^{-3}	-	6.8×10^{-3}[18]	-
	r_{41}	1.407×10^{-3}	-	-	1.563×10^{-3}
Δ_μ ($^\circ\mathrm{C}^{-1}$)	r_{63}	-0.248×10^{-3}	-	-0.41×10^{-3}[18]	-
	r_{41}	-0.473×10^{-3}	-	-	-0.554×10^{-3}

Moreover, from Eqs. (12a), (12d), (16), and (18), we can deduce that $\rho_\mathrm{trans} < \rho_\mathrm{long}$ and $\xi_\mathrm{m,trans} < \xi_\mathrm{m,long}$, which means that the transverse EO-modulation system is better than its homologous longitudinal EO-modulation system.

6. Summary and conclusion

The first part of the present work is dedicated to introducing and analyzing the concept of opto-electrical bias $\bar{\varphi}$ in an EO-modulation system. Next, we deal with corresponding questions of thermal instability, as expressed by various TO or temperature-dependence parameters. It is thus proven that the choice of a transverse or a longitudinal configuration in the system may more or less affect the above parameters and modify the thermal stability of the EO crystal and the entire system as well. In addition, we derive a number of basic equations with which one can investigate the effect of temperature on the TO and other temperature-dependence parameters in both transverse and longitudinal EO-modulation systems. A comparison between these two configurations as regards the TO behaviour of the EO crystal and the entire system is also discussed.

Finally, it is concluded with a discussion about the accuracy and reliability of the obtained result on r, and its temperature dependence, along with comments on the comparison of the present cut KDP crystal (involving the r_{63} transverse configuration) with other orientations such as 45° Z-cut KDP crystal. For this comparison, a TO coefficient $\mathrm{d}\Delta n^{(0)}/\mathrm{d}T$ of spontaneous birefringence is found to be smaller in our crystal orientation than its Z-cut KDP-counterpart[18]. By contrast, it is ascertained that at the output of the entire EO-modulation system in the case of our crystal orientation, the IM depth m will possess a temperature coefficient ξ_m and a TO coefficient $\mathrm{d}m/\mathrm{d}T$ much lower (∼50 times) than in the case of a Z-cut KDP crystal. In conclusion, our results provide a highly improved thermal stability to the system's IM depth, which is in a fact of primary importance.

References

1. A. Rauber, in *Current Topics in Material Sciences* E. Kaldis, (ed.) (North Holland, Amsterdam, 1978).
2. F.-S. Chen, Proc. IEEE **58,** 1440 (1970).
3. H. L. Saadon, N. Théofanous, M. Aillerie, and M. D. Fontana, Appl. Phys. B **83,** 609 (2006).
4. I. P. Kaminow and E. H. Turner, Proc. IEEE **54,** 1374 (1966).
5. M. Aillerie, N. Théofanous, and M. D. Fontana, Appl. Phys. B **70,** 317 (2000).
6. N. Theofanous, M. Aillerie, M. D. Fontana, and G. E. Alexakis, Rev. Sci. Instrum. **68,** 2138 (1997).
7. D. Eimerl, IEEE J. Quantum Electron. **23,** 2104 (1987).
8. R. M. A. Azzam and N. M. Bashara, *Ellipsometry and Polarized Light* (2nd edn.) (North Holand, Amsterdam, 1989).
9. T. S. Narasimhamurty, *Photoelasticity and Electro-Optic Properties of Crystals* (1st edn.) (Plenum, New York, 1981).
10. P. S. Theocaris and E. E. Gdoutos, *Matrix Theory of Photoelasticity* (Springer-Verlag, Berlin, 1979).
11. L. Guilbert, J. P. Salvestrini, H. Hassan, and M. D. Fontana, IEEE J. Quantum Electron. **35,** 273 (1999).
12. W. R. Cook, Jr., J. Appl. Phys. **38,** 1637 (1967).
13. I. P. Kaminow, *An Introduction to Electro-Optic Devices* (Academic Press, New York and London, 1974).
14. G. W. C. Kaye and T. H. Laby, *Tables of Physical and Chemical Constants* (Longman Group Ltd., London, 1995).
15. E. N. Volkova and I. A. Velichko, Sov. Phys.-Crystallogr. **18,** 256 (1973).
16. N. Theofanous, IEEE J. Quantum Electron. **8,** 507 (1976).

17. M. Aillerie, "Comparison between different methods for electro-optic measurements: application in $LiNbO_3$" (in French) PhD Thesis (Metz University, France, 1991).
18. F. Abdi, M. Aillerie, M. D. Fontana, B. Wgncke, and F. Brehat, Opt. Quantum Electron. **29,** 441 (1997).
19. R. A. Philips, J. Opt. Soc. Am. **56,** 629 (1966).

Appendix A: Effect of temperature on the EO coefficient r

By derivation of Eq. (7), we have

$$\frac{\mathrm{d}r}{\mathrm{d}T} = \frac{\mathrm{d}}{\mathrm{d}T}\left(\frac{\lambda}{2n^3V_\pi}\right) = \frac{\lambda}{2}\left[\frac{1}{V_\pi}\frac{\mathrm{d}}{\mathrm{d}T}\left(\frac{1}{n^3}\right) + \frac{1}{n^3}\frac{\mathrm{d}}{\mathrm{d}T}\left(\frac{1}{V_\pi}\right)\right]. \quad (A.1)$$

Formula (A.1) can be written as

$$\rho = \frac{1}{r}\frac{\mathrm{d}r}{\mathrm{d}T} = -\frac{3}{n}\frac{\mathrm{d}n}{\mathrm{d}T} - \frac{1}{V_\pi}\frac{\mathrm{d}V_\pi}{\mathrm{d}T}, \quad (A.2)$$

where $\beta=(1/n)(\mathrm{d}n/\mathrm{d}T)=\gamma$, $n = (2n_0^2n_\mathrm{e}^2/(n_0^2+n_\mathrm{e}^2))^{1/2}$, and $\delta=(1/\mathrm{V}_\pi)(\mathrm{dV}_\pi/\mathrm{d}T)$. Formula (A.2) can be written as

$$\rho = -(\delta + 3\gamma). \quad (A.3)$$

Appendix B: Equation for the coefficient γ

Using Eq. (4), we obtain

$$\begin{aligned}\frac{\mathrm{d}n}{\mathrm{d}T} &= \sqrt{2}\Bigg[-\frac{1}{2}(n_0n_\mathrm{e})(n_0^2+n_\mathrm{e}^2)^{-3/2}\left(2n_0\frac{\mathrm{d}n_0}{\mathrm{d}T} + 2n_\mathrm{e}\frac{\mathrm{d}n_\mathrm{e}}{\mathrm{d}T}\right) \\ &\quad + (n_0^2+n_\mathrm{e}^2)^{-1/2}\left(n_0\frac{\mathrm{d}n_\mathrm{e}}{\mathrm{d}T}n_\mathrm{e}\frac{\mathrm{d}n_0}{\mathrm{d}T}\right)\Bigg] \\ &= \frac{\sqrt{2}}{\sqrt{n_0^2+n_\mathrm{e}^2}}\Bigg\{\frac{-n_0n_\mathrm{e}}{(n_0^2+n_\mathrm{e}^2)}\left[n_0\frac{\mathrm{d}n_0}{\mathrm{d}T} + n_\mathrm{e}\frac{\mathrm{d}n_\mathrm{e}}{\mathrm{d}T}\right] \\ &\quad + \left[n_0\frac{\mathrm{d}n_\mathrm{e}}{\mathrm{d}T} + n_\mathrm{e}\frac{dn_0}{\mathrm{d}T}\right]\Bigg\}. \quad (B.1)\end{aligned}$$

Formula (B.1) can be given by

$$\beta = \frac{1}{n}\frac{\mathrm{d}n}{\mathrm{d}T} = \frac{n_0^2\beta_\mathrm{e} + n_\mathrm{e}^2\beta_0}{n_0^2+n_\mathrm{e}^2} = \gamma, \quad (B.2)$$

where $\beta_0=(1/n_0)(\mathrm{d}n_0/\mathrm{d}T)$ and $\beta_\mathrm{e}=(1/n_\mathrm{e})(\mathrm{d}n_\mathrm{e}/\mathrm{d}T)$.